REFINED THERMAL FLOW SENSORS BY TRANSDUCTION ENGINEERING

F. Kohl[1]*, F. Keplinger[2], R. Beigelbeck[1], J. Kuntner[2], J. Schalko[2], A. Jachimowicz[2]
[1]Research Unit for Integrated Sensor Systems, Austrian Academy of Sciences, Austria
[2]Institute of Sensor and Actuator Systems, Vienna University of Technology, Austria

*Corresponding author: Franz Kohl, Phone +432622/2342021, Fax +432622/2342099
e-mail: franz.kohl@oeaw.ac.at

Abstract: Miniaturized flow sensors composed of a thin membrane supporting appropriately positioned heating resistors and temperature sensors were studied by computer-numeric analysis. Significant improvements of the steady-flow transduction characteristics as well as the responses to step-like changes of the dissipated power are feasible by design modifications and new transduction schemes.
Keywords: Thermal flow sensors, micromachined devices, calorimetric flow sensors

INTRODUCTION

Calorimetric flow sensors are preferable devices for limited space applications in mass products like cars or domestic appliances. They are well-known for ruggedness, sensitivity, and fast response, each of which may be achieved using MEMS technologies. After a brief description of state of the art designs, we discuss new concepts enabling faster response, enhanced transduction efficiency, improved durability, as well as means for in-service monitoring of the functionality.

PRINCIPLE AND STATE OF THE ART

Calorimetric flow sensors rely on flow dependent heat transfer altering the temperature distribution close to a small heat source. The temperature field is probed at a few pre-selected sites. Based on these recordings, a representative characteristic of the flow field is determined using suitable calibration information. The cross sectional view depicted in Fig. 1 is typical for the majority of micromachined versions of calorimetric flow sensors. The heating resistor H generates a temperature profile in the membrane and the surrounding fluid. Due to convective heat transport, the profile is altered if the fluid flows along the membrane surface as indicated. Local changes of the temperature profile are probed using the thermistors MT1 and MT2. Flow related information can be derived from different variations of their temperatures, (T_{MT1}−T_{MT2}), wherein the subscripts indicate the measuring site. In contrast to hot-wire and hot-film anemometers, calorimetric sensors offer flow direction information in principle. More refined structures employ larger one-dimensional arrays of temperature sensors to optimize the sensitivity over a wide measuring range [1], whereas two-dimensional arrangements of these components are used to gain directional resolution [2]. To achieve high sensitivity and fast response, all essential components are made by thin film technology and they are embedded in a extremely thin membrane.

Thermistors based on semiconducting films are favorable temperature sensors for calorimetric sensing. Their main advantages comprise high temperature resolution, miniaturization potential, and variability of shape. Furthermore, low operating currents can be achieved based on materials that exhibit a high specific resistivity. This enables small-sized interconnecting lines causing low parasitic thermal conductances.

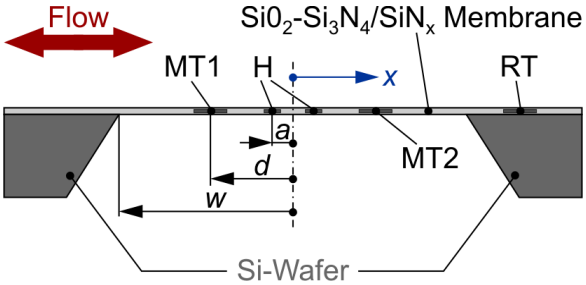

Fig. 1. Schematic cross section of a typical calorimetric flow sensor design.

Figure 2 depicts the usual placement of thin film components on the membrane which measures 1 mm in length and 0.5 mm in width, for example. A KOH based anisotropic wet etch process and backside lithography is used to shape this membrane. A closer examination of the pattern reveals a 10 µm misalignment caused introduced by the backside lithography step. Further details of the technology and key specifications of such sensors are given elsewhere [3, 4]. The distances a, d, and w (indicated in Fig. 1) measure 10 µm, 140 µm, and 250 µm, respectively. This spacing resemble a compromise between high sensitivity and speed of response [4].

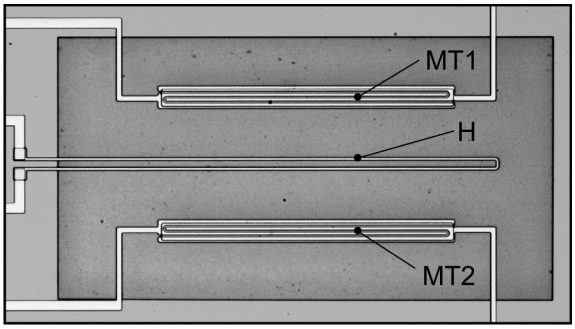

Fig. 2. Top view of the membrane area of a flow sensor featuring a common layout. Highest sensitivity is achieved for top down orientated flows. This orientation coincides with the flow direction indicated in Figure 1.

Thermal flow sensors may be operated with constant power (CP mode) or with a constant tempera-

ture offset between heating resistor and the supplied fluid (CT mode). The fluid temperature is measured with a reference sensor RT located at the silicon frame. For high flow velocities, the CP operating mode is inappropriate. In this regime $|T_{MT1}-T_{MT2}|$ decreases with increasing flow. Still, the asymmetry of the temperature distribution steadily increases with increasing flow. However, this effect is overcompensated by the intensification of convective heat dissipation which lead to a general reduction of the excess temperatures throughout the membrane area [5, 6]. Accordingly, the slope of the $(T_{MT1}-T_{MT2})$-versus-flow-characteristic reverses its sign. Hence, the flow concluded from the sensor signal of the CP mode may be ambiguous. For calorimetric flow sensors, an enhanced version of the CT operating mode is feasible keeping the mean of the temperatures of MT1 and MT2 a fixed amount above the fluid temperature T_{RT}. Thus $\Delta T = 0.5\cdot(T_{MT1}+T_{MT2}) - T_{RT}$ is kept constant. This is a very convenient approach since T_{MT1} and T_{MT2} are already available with high accuracy. In contrast, deriving the precise heater temperature from resistance measurements is a very ambitious task as the heating resistor serves also as a closed-loop controlled thermal actuator. Furthermore, the enhanced CT mode offers a better transduction, $|T_{MT1}-T_{MT2}|$ versus flow than the standard CT mode as outlined below.

METHOD

We investigated state of the art air-flow sensors and the progress achievable by design improvements using finite element (FE) computations. The analysis is based on a two-dimensional (2D) FE model corresponding to the cross section shown in Fig. 1. The results presented below were obtained using COMSOL Multiphysics. The detailed patterns of thin film device cross-sections were approximated by rectangular areas of equal size and average thermal parameters, which are embedded within the membrane. Based on the Navier-Stokes equations for incompressible fluids, air-flow velocity fields were calculated approximately. The temperature dependencies of fluid viscosity, density, heat capacity and thermal conductivity were left out of consideration. Thus the effects of natural convection are neglected throughout the model. To reduce the computational effort, a uniform flow profile is assumed at the model inlet, which is situated 0.5 mm upstream of the heater. Due to the sticking of the fluid at the sensor surface, typical flow boundary layers emerge, as Fig. 3 exemplifies. This approach yields the smallest thickness of the flow boundary layer achievable with a sensor chip measuring 1 mm in the direction of flow. However, this simplification ignores the fluid displacement due to the finite thickness of the sensor chip, which would inevitably occur if the bare flow sensor chip is inserted into a homogeneous flow field.

All computed FEM results are in good agreement with experiments [3, 4]. Hence, the 2D FEM analysis is an appropriate tool to predict the behavior of new sensors designs.

Four main areas of significant improvement of the performance of common calorimetric flow sensors were identified, which can be achieved by design modifications and modified transduction schemes, i.e., without any change of technological processes.

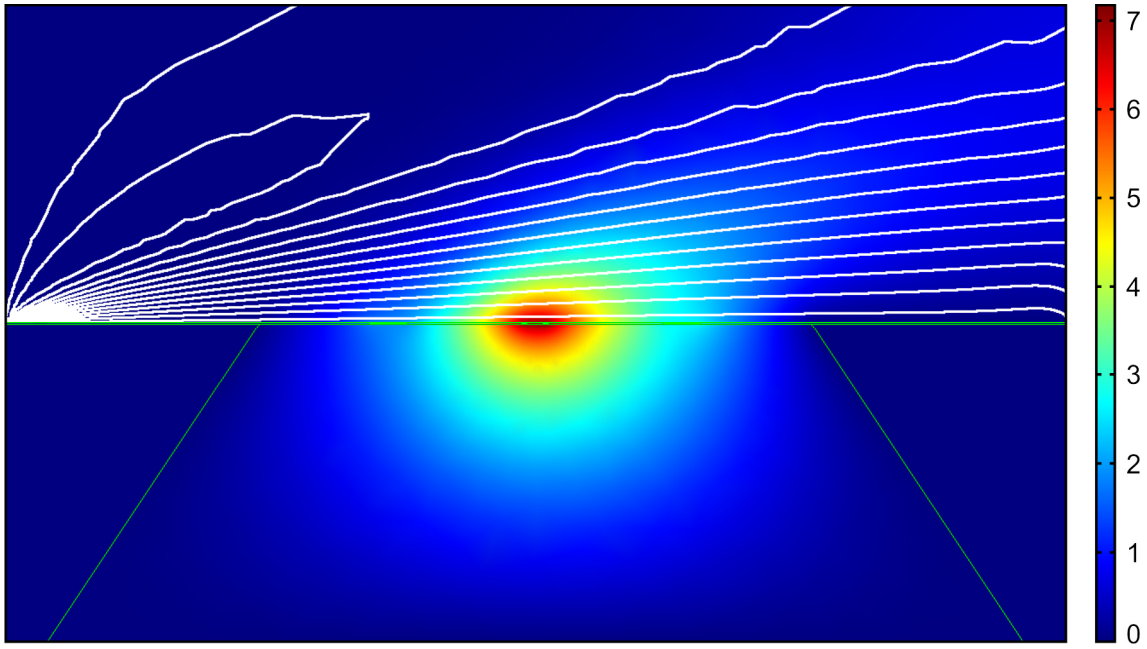

Fig.3: Temperature field for a uniform air inflow of 1m/s and an operating power of 0.5 mW. The 2D model measures 1 mm parallel and 0.6 mm perpendicular to the sensor surface. Fluid flow takes place in the upper half of the model as indicated by the isotachs of the flow profile (increment 0.2 m/s). The bottom half is composed of the wedge shaped micromachined Si substrate at both sides, and a compartment underneath the membrane, which is filled with still air. For the lower half of the model all boundaries at the outline are kept at zero excess temperature. The color coded excess temperatures range from 0 K (dark blue) to about 7 K (dark red), where the temperature at the air inflow is used as a the reference level.

These fields are (i) improved sensor dynamics, (ii) reduction of the thermal stress acting on the sensor membrane, (iii) improvement of existing tools and new possibilities for in-service operability checks, and (iv) removal of the saturation of the transduction characteristics at very high flow velocities.

FEATURES OF THE COMMON DESIGN

Figure 3 shows computed temperature profiles of the enhanced CT mode for the indicated set of free-field air velocities. All curves of the diagram are normalized to $\Delta T = 1$. It can be seen that the maximum of the temperature offset is located near the downstream heater trace. It grows with raising flow velocity by a factor of three up to the sevenfold of ΔT. Compared to the standard CT mode, the enhanced CT mode offers a higher thermal output $|T_{MT1} - T_{MT2}|$ by the same factor. The thermal stress induced by the enhanced CT flow sensor operation is significantly higher.

The operating power needed to keep ΔT constant is considerably higher than the power which would be required to establish a constant heater excess temperature that equals ΔT. The higher power consumption of the enhanced CT mode may be understood as follows. Heat input to a volume element of the membrane is mainly established by heat conduction within the membrane. The related thermal conductance, however, decreases with increasing distance from the heater. In contrast, convective heat transfer to the fluid is most efficient where surface temperatures increase with respect to the direction of flow, i.e., in the region upstream of the heater. Hence, the larger the distance from the heater, the more heating power is needed to establish a specified excess temperature.

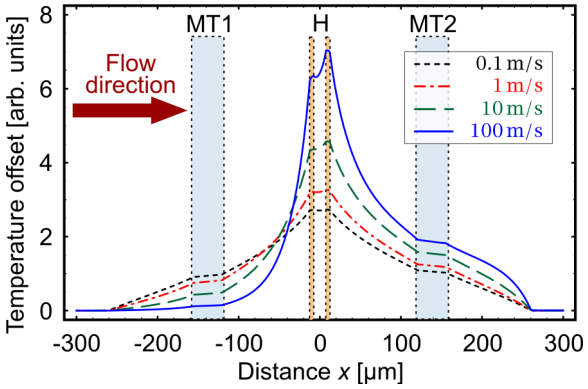

Fig. 3. Temperature profiles across the membrane region of a flow sensor (standard design) when operating in the enhanced CT mode.

Figure 3 reveals also that at very high flow rates upstream temperatures approach the temperature of the incoming fluid whereas the excess temperature of the downstream approximates $2 \cdot \Delta T$. Consequently, the thermal output at very high flow velocities saturates at $|T_{MT1} - T_{MT2}| \rightarrow 2 \cdot \Delta T$.

ADVANCED TRANSDUCTION SCHEME

With the arrangement of components on the membrane shown in Fig. 4, the specifications and monitoring capabilities can be significantly improved. It employs two heating resistors. An additional thermistor is placed in the centre of the membrane area. The membrane sizes of Fig. 3 and Fig. 2. coincide. Based on two separated heaters, new transduction schemes become feasible [7], which are out of scope for this contribution. The redundancy of components enables also advanced fault diagnostic strategies.

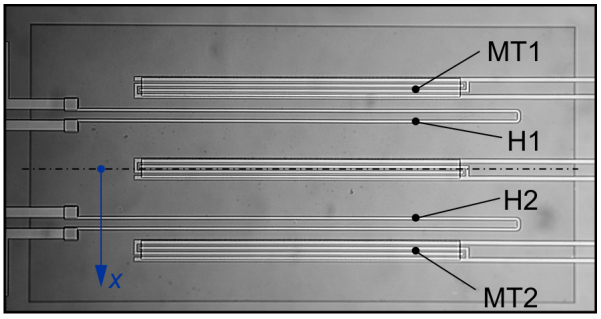

Fig. 4. Top view of the membrane area of a fabricated flow sensor as an example of an improved design. Two equal-valued heating resistors are used for flow sensing together with the top and bottom thermistors.

For the sake of compatibility, we make use of MT1 and MT2 only and consider a simple series connection of equal valued heating resistors, i.e., equal amounts of dissipated power.

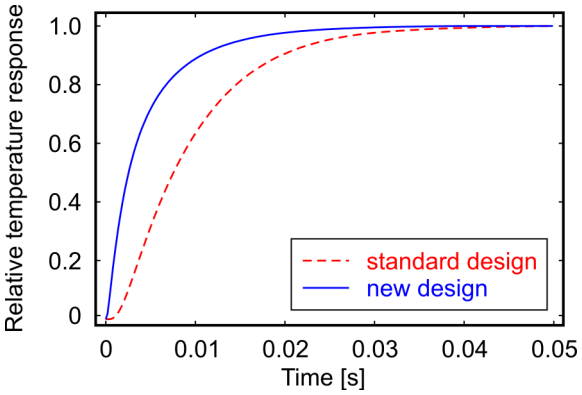

Fig. 5. Zero-flow temperature sensor response to step like changes of the power dissipated by the neighboring heater.

The thermal delay between heater and membrane temperature sensor limits the achievable performance of the control loop employed by the enhanced CT operational mode. The calculated responses to step-like changes of the heating power are shown in Fig. 5 for both designs. These transients can be modeled by overdamped second-order systems with dead time. The fit parameters of the transients are listed in Table 1 for both design cases.

Table1. Transient response parameters.

Parameter [ms]	Standard design	Improved design
τ_1	7.7	4.3
τ_2	1.5	< 0.1
Dead time	0.5	< 0.1

Due to the smaller distance between adjacent heater and thermistor, the new sensor design exhibits significantly lower delays. For the enhanced CT operation mode, a much faster response to sudden flow changes can be achieved with the new design.

CT operating modes are based on closed loop control of temperature(s) at specific site(s) on the membrane by means of the heating resistor. On principle, these operation modes enable continuous monitoring of the functionality of the heating resistors and the temperature sensors. In case of high flow velocities and a standard design, the temperature response to variations of the heating power becomes very small at the site of MT1. Thus, an in-service check of the functionality of the upstream temperature sensor is hindered considerably.

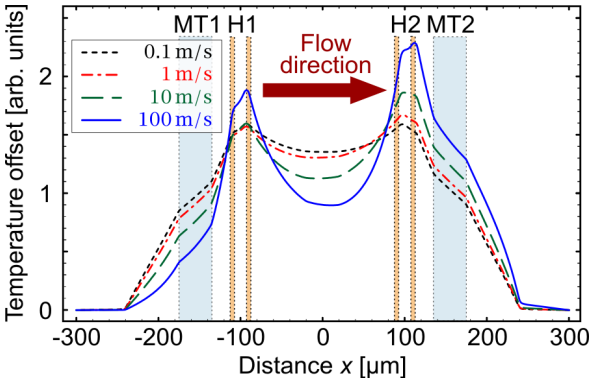

Fig. 6. Temperature profiles along the membrane for an improved sensor design.

Figure 6 depicts stationary temperature profiles calculated for the enhanced CT mode and the improved sensor layout.

The improved design provides a much larger excess temperature at the upstream thermistor site. Moreover, this marked improvement is obtained in spite of the moderate maximum excess temperature of $2.3 \cdot \Delta T$. Thus the functionality of MT1 can easily be monitored during sensor operation, e.g., by superimposing a small variation upon the bias power and the detection of related temperature variations.

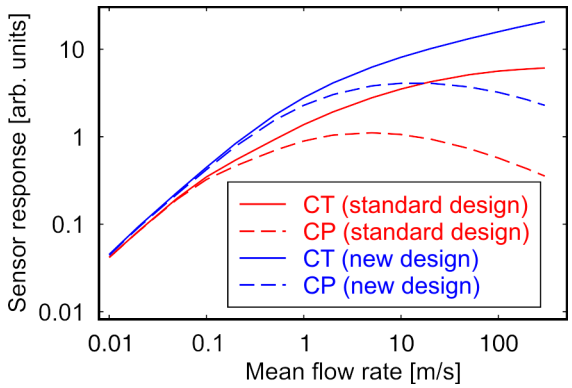

Fig. 7. Comparison of flow responses calculated for each sensor design and two operating modes.

The sensor characteristics of the standard and the advanced design are shown in Fig. 7 for both, the CP and the enhanced CT mode. The characteristics of the new design are shifted up by a factor of two approximately to coincide with those of the standard design at low flow velocities. The reduced useful transduction range of the CP mode due to the non-monotonous characteristics becomes obvious. As outlined above, the transduction characteristic of the standard sensor design saturates at high flow velocities even in the enhanced CT mode. Due to the closer spacing of heater and neighboring temperature sensor, the saturation of the transduction characteristic of the improved design occurs beyond the investigated flow range. In terms of resolution at high flow velocities the new design outperforms the conventional device significantly.

CONCLUSION

FEM analysis of calorimetric flow sensors proved that faster response, extended measuring range, reduced thermal load, and improved in-service functionality monitoring is obtainable at the same time through more sophisticated arrangements of heat sources and temperature sensors on the sensor membrane.

ACKNOWLEDGEMENT

We greatly acknowledge partial support of this work by the Austrian Science Fund, FWF, and the Society for Micro- and Nanoelectronics, GMe.

REFERENCES

1. N. Sabaté, J. Santander, L. Fonseca, I. Gràcia, C. Cané, Multi-range silicon micromachined flow sensor, *Sensors and Actuators* A. Vol. 110 (2004) pp 282–288.
2. S. Kim, S. Nam, S. Park, “Measurement of flow direction and velocity using a micromachined flow sensor”, *Sensors and Actuators* A, Vol. 114 (2004) pp 312–318.
3. A. Glaninger, A. Jachimowicz, F. Kohl, R. Chabicovsky, G. Urban, Wide range semiconductor flow sensors, *Sensors and Actuators* A, Vol. 85 (2000) pp 139–146.
4. F. Kohl, R. Fasching, F. Keplinger, R. Chabicovsky, A. Jachimowicz, G. Urban, Development of miniaturized semiconductor flow sensors, *Measurement,* Vol. 33 (2003) pp 109–119.
5. A. Rasmussen, C. Mavriplis, M.E. Zaghloul, O. Mikulchenko, K. Mayaram, Simulation and optimization of a microfluidic flow sensor, *Sensors and Actuators* A, Vol. 88 (2001) pp121-132.
6. H. Ernst, A. Jachimowicz, G.A. Urban, High resolution flow characterization in Bio-MEMS, *Sensors and Actuators* A, Vol. 100 (2002) pp 54–62.
7. T.S.J. Lammerink et al., A New Class of Thermal Flow Sensors Using DT=O as aControl Signal, *Proceedings of the 13th Annual International Conference on Micro Electro Mechanical Systems* (2000), pp 525–530.